

The Periodic Standing-Wave Approximation: Overview and Three Dimensional Scalar Models

Zeferino Andrade¹, Christopher Beetle¹, Alexey Blinov¹, Benjamin Bromley¹,
Lior M. Burko¹, Maria Cranor¹, Robert Owen^{1,2}, and Richard H. Price¹
¹*Department of Physics, University of Utah, Salt Lake City, Utah 84112,*
²*Theoretical Astrophysics, California Institute of Technology, Pasadena, CA 91125*

Abstract

The periodic standing-wave method for binary inspiral computes the exact numerical solution for periodic binary motion with standing gravitational waves, and uses it as an approximation to slow binary inspiral with outgoing waves. Important features of this method presented here are: (i) the mathematical nature of the “mixed” partial differential equations to be solved, (ii) the meaning of standing waves in the method, (iii) computational difficulties, and (iv) the “effective linearity” that ultimately justifies the approximation. The method is applied to three dimensional nonlinear scalar model problems, and the numerical results are used to demonstrate extraction of the outgoing solution from the standing-wave solution, and the role of effective linearity.

PACS numbers: 04.25.Dm,04.30.Db,04.25-g,02.60.Lj

I. INTRODUCTION

Background

The inspiral and merger of a binary pair of compact objects (holes or neutron stars) is one of the most promising sources of signals detectable by gravitational wave observatories. For the ground-based detectors LIGO[1], VIRGO[2], GEO600[3] and TAMA[4], binary merger, especially of intermediate-mass black holes[5] is an exciting possibility; for the space-based LISA detector[6, 7], the detection of inspiral/merger of supermassive holes is highly probable, and is one of the primary scientific targets.

The need for theoretical waveforms for the inspiral/merger has driven the effort to find a computational solution for the details of the process, but the difficulty of the task has made this problem also a measure of the usefulness of numerical computation in general relativity. The hope has been that numerical codes evolving initial data can compute the orbital motion using Einstein’s equations and, in the case of neutron stars, using hydrodynamical equations. These evolution codes would have, as an intrinsic feature, the loss of energy by the binary due to outgoing wave energy, and the gradual inspiral due to this loss.

An important reason for the limited progress on this problem is the matter of timescales. Near a black hole, the timescale on which the gravitational field can change is GM/c^3 , where M is the mass of the hole; for a neutron star the timescale is several times longer. The time step in evolution codes is governed by this short timescale. (More precisely, the spatial grid near the compact objects must be smaller than GM/c^2 , and to satisfy the Courant condition, the time step must be no larger than $1/c$ times this grid size.) By contrast, the timescale $\sqrt{r^3/GM}$, for orbital motion at radius r , is much larger than this, and the timescale for the interesting dynamics, the radiation-reaction driven inspiral is much greater yet. The consequence of this incompatibility of timescales is that a very large number of time steps is needed in order to see the physics of interest. And computing a large number of time steps is not yet possible. Instabilities[8, 9] operating at the short timescale prevent the code from giving useful answers about the long timescale.

The origin of the difficulty suggests its cure: an approximation method that avoids the short timescales. Here we describe such a method: a solution for periodic sources and fields. We assume that the compact objects, and their fields, rotate with a constant angular velocity (to be denoted Ω below.) This approximation will fail of course, in the very latest stages of inspiral merger, when the orbit decays rapidly due to a secular instability or the dynamics of the final merger. But that last stage is, by its very nature, rapid; its timescale is only several times that of the shortest timescale of the problem. This last stage, then, can plausibly be handled by numerical evolution codes. Indeed, evolution codes, especially with perturbation theory handling the final ringdown[10], are already near to doing this. Our goal, then, is a method that can approximate the solution up to the time that numerical evolution codes can take over the task that only they can handle. Our approach is not entirely new; it is similar in underlying motivation to a method introduced by Detweiler and collaborators[11, 12], but our approach is very different in its details and its implementation. It is also very closely related to the approach being used by Friedman and his collaborators[13].

Periodic motion and outgoing waves are, of course, impossible in Einstein's theory, both intuitively and mathematically¹. For this reason, we will solve for standing waves (to be defined and discussed below) in the gravitational field. Our periodic standing-wave (PSW) approach, then, will be to find exact (numerical) periodic standing-wave solutions of the Einstein field equations and to use these exact solutions as approximations to the physical problem of slow inspiral with outgoing waves.

The most basic ideas behind this periodic standing-wave solution have already been introduced in a previous paper[15], but the implementation there was applied only to two-dimensional models and was limited in other ways; in particular, that paper did not discuss the general meaning of standing waves. Here we present a more general discussion, along with numerical results for three-dimensional models. This paper is meant to serve as the introduction to the PSW, with subsequent papers presenting more detailed information on particular methods, and progress on solving the physical problem.

Effective linearity and uses of the method

A key idea in our approach is the relationship of standing waves to outgoing waves. In a linear field theory, a definition of standing waves is that they are half the sum of an outgoing solution and ingoing solution. Here, as in Ref. [15], we shall call this sum LSIO for linear superposition of (half) ingoing and (half) outgoing solutions. In a linear theory, such a superposition is itself a solution. In our nonlinear field model theories, it will turn out that — despite strong nonlinearities — this continues to be very nearly true. This *effective linearity*, the approximate equality of the LSIO and a true standing-wave solution, has already been demonstrated for simple two-dimensional models, and results for three dimensional nonlinear models will be presented below. More important, the basis for effective linearity appears to be robust. This basis lies in the fact that the strong nonlinearities in our model theories (and in the physical problem) are confined to the near-field regions around the sources. In these nonlinear near-field regions the solution is insensitive to the distant boundary conditions; it is substantially the same for ingoing boundary conditions as for outgoing. In this near-field region then, the LSIO will be very nearly a solution despite strong nonlinearities, since we are superposing nearly identical solutions. Outside this strong-field near zone the model theories, and the physical theory, are nearly linear, so that again the LSIO is a solution. The LSIO will therefore be a good approximation to a solution everywhere.

Below, we shall choose our definitions of standing-wave solution to be close to that of a LSIO, and our approximation to a large extent is based on interpreting a standing-wave solution to be approximately a LSIO. In the weak field region this LSIO can be deconstructed into outgoing and ingoing pieces and this deconstruction can be continued to the strong field source region. (In the source region, the outgoing piece is simply half the solution.) By doubling the outgoing piece thus extracted from the standing-wave solution, we thereby arrive at an approximation to the outgoing solution for a nonlinear problem. It is in this manner that we will extract an approximation of an outgoing solution from a computed standing-wave solution.

This is an appropriate place to point out, though not for the last time, the importance of model problems. In Einstein's theory there is no obvious meaning to the periodic outgoing solution, so one cannot make statements about it, let alone carry out numerical studies. Statements and computations *are* possible for nonlinear model problems, so that tests of effective linearity with such models are crucial.

The outgoing solutions extracted from our exact periodic solutions can serve two purposes. First, we can use a quasistationary sequence of outgoing approximations as a model for the slow physical inspiral. In this approach the mass of the system, measured in a weak wave zone far from the orbiting sources, decreases due to the loss of energy in outgoing radiation. When we find the system energy as a function of orbit radius, and we compute the outgoing radiation, we can infer the rate at which the orbital radius decreases. The difficulty, as with any such quasistationary sequence, is how to know that we are comparing the "same" system at different radii. In the case of neutron star's the answer is clear; baryon number is an unchanging tag that identifies neutron stars to be the same. For black holes, the equivalent tag would be some local mass. The concept of an isolated horizon[16] might give us that local mass.

The second use for our extracted outgoing solutions is to provide initial data for evolution codes. A spacelike slice of our extracted outgoing field will be an excellent approximation to the physical initial data, and should be very nearly a solution to the initial value equations. With little change our extracted outgoing initial data, can be made into exact (numerical) initial data through the use of York's decomposition[17, 18].

¹ A periodic binary would have no secular change in its energy, but gravitational waves intuitively remove energy. This argument can be made mathematically complete using the conservation law for $H^{\alpha\beta\mu\nu}$, as defined in Misner *et al.*[14].

These two purposes of our solution are not distinct. The natural end point for a quasistationary sequence of PSW solutions is the “last orbit,” the final stage of motion at almost constant radius. This stage may end due to a secular instability, like that of a particle in a black hole spacetime, or due to the imminence of the merger, the formation of the final black hole. In either case, this end point must be handled by a numerical evolution code, and in either case, the quasistationary sequence will provide ideal initial data for the continuation of the problem by numerical evolution.

The nature of the mathematical problem

In the standard approach to computing binary inspiral, initial data are evolved forward in time. In our approach, with periodic symmetry imposed, there is no evolution in the usual sense, and there is not the usual concept of initial data. Rather we must satisfy boundary conditions at large radius: outgoing, ingoing or standing-wave boundary conditions in model problems, and only standing-wave conditions in general relativity. The boundary value problems that we must solve differ in two important ways from common boundary value problems. First, our partial differential equations (PDEs) are of *mixed* type. They are of elliptical character in some regions and hyperbolic character in others; this will be particularly clear in the model problem to be presented below. We will argue that the mixed character causes no fundamental difficulty, and will demonstrate this with the model problems. The mixed character, however, does complicate the use of some of the most efficient numerical means of solving boundary value problems. Second, we must define what we mean by “standing-wave boundary conditions.” Unlike outgoing and ingoing conditions, there is no simple local condition corresponding to what we will mean by standing waves in a nonlinear problem. We will present two fundamentally different candidates for the standing-wave condition, and here will present results of computations with one those of those two choices. (The alternative choice of standing-wave condition is best implemented with a special numerical method, and will be presented elsewhere[19].)

Stepping back from such details, one may be led to ask more fundamental questions about the whole approach. Such questions arise especially because the PSW spacetime we compute has some awkward features. Since the exact PSW solution contains an infinite amount of gravitational wave radiation, it cannot be expected to meet the asymptotic flatness conditions of the theorems about the fall-off of fields. But the spacetime *is* asymptotically flat in that the spacetime curvature decreases with increasing distance from the binary source. Another sign that the PSW spacetime has rough edges is that it must not have regular null infinities; Gibbons and Stewart[20] have shown that spacetimes with well-behaved Scri^+ and Scri^- cannot be periodic.

It is useful, before diving into details, to clarify what the relationship is between the slightly singular spacetime we will be computing, and the physical problem that really interests us. To make this connection we can think of the binary system going through several orbits at almost constant radius. A weak wave zone exists at some distance from the orbit during this epoch of the motion. The stippled region in Fig. 1 shows the relevant region as part of the larger physical spacetime. In this limited region the source motion and the fields are almost periodic, and it is in this region only that we hope to approximate the physical fields by the outgoing fields extracted from the computed PSW solution. The imperfect asymptotic structure of the PSW spacetime is therefore irrelevant to its physical usefulness.

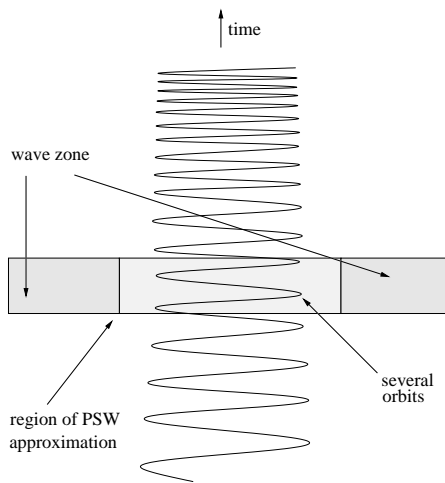


FIG. 1: The PSW solution is meant to be an approximation to the physical spacetime only in a limited region.

In the remainder of this paper we will first present, in Sec. II, the mathematical details of a nonlinear model with which we clarify many aspects of the PSW approximation. We then discuss, in Sec. III, the numerical methods needed

to find PSW solutions, especially those aspects of the numerical methods that are idiosyncratic to the special features (mixed character, standing-wave boundary conditions, nonlinearities) of our problem. In this section also, results are presented of the numerical methods. The results are discussed, and put into the context of the next steps in this project[19], in Sec. IV.

II. PERIODIC SOLUTIONS, STANDING WAVES, AND MODEL PROBLEMS

Mixed PDEs and well-posedness

As stated above, we seek a solution to Einstein's equations in which the sources and the fields rotate rigidly. The mathematical statement of this rigid rotation is that there is a helical Killing vector, a Killing vector that is timelike close to the sources and spacelike far from the sources. (For more on helical Killing symmetry see Ref. [21].) For fields in flat spacetime our Killing vector $\vec{\xi}$ takes the form

$$\vec{\xi} = \partial_t + \Omega \partial_\phi \quad (1)$$

in spherical or cylindrical spatial coordinates, and

$$\vec{\xi} = \partial_t + \Omega (x\partial_y - y\partial_x) \quad (2)$$

in Cartesian spatial coordinates. The parameter Ω , which must be a constant, can be thought of as the rotation rate of the source and fields with respect to an inertial reference frame. For the flat spacetime case, the null surface $\vec{\xi} \cdot \vec{\xi} = 0$ is a cylinder of radius $1/\Omega$ coaxial with the rotation axis. (Here and below we use units in which $G = c = 1$.) This cylinder separates the inner region of timelike $\vec{\xi}$ from the outer region of spacelike $\vec{\xi}$, as shown in Fig. 2. Since this surface, in a sense, represents the points at which the rigidly rotating fields are moving at c , we call this surface the ‘‘light cylinder,’’ in analogy with pulsar electrodynamics.

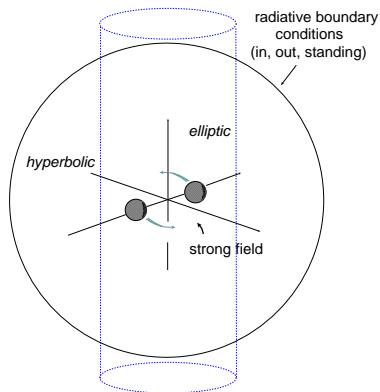


FIG. 2: The ‘‘light cylinder’’ separating the elliptic and hyperbolic regions of the problem intersects the large spherical surface on which numerical boundary conditions are imposed.

One immediate advantage of the helical symmetry is that it reduces the number of independent variables, thereby greatly reducing the computational difficulty of a problem. In our simple flat spacetime models this reduction is most easily understood by the fact that helically symmetric scalars cannot depend in an arbitrary way on the spherical Minkowski coordinates t, r, θ, ϕ but can depend only on t and ϕ in the combination $\varphi \equiv \phi - \Omega t$. Thus, in the t, r, θ, φ system the Killing vector is $\vec{\xi} = \partial_t$. These ideas are clarified with a simple flat spacetime model theory for a scalar field Ψ

$$\Psi_{;\alpha;\beta} g^{\alpha\beta} + \lambda F = S. \quad (3)$$

The term $F(\Psi, x^\alpha)$ is included to allow for nonlinearity; the constant λ adjusts the strength of the nonlinearity. In order for a helically symmetric solution Ψ to exist, the explicit coordinate dependence of F must be compatible with the symmetry. That is, F can have explicit coordinate dependence only on r, θ , and φ . The most natural choice for a model would be one in which there is no coordinate dependence, one in which the background spacetime is featureless.

We include the possibility of spatial dependence for convenience below. Changing the spatial dependence will help to clarify the accuracy of the PSW approximation when nonlinearities are important.

In the application of the PSW method to holes, an inner boundary condition will be used at a small, approximately spherical surface. For simplicity here, however, we use an explicit source term,

$$S = \frac{\delta(r-a)}{a^2} \delta(\theta - \pi/2) [\delta(\varphi) + \delta(\varphi - \pi)] , \quad (4)$$

representing two points, each of unit scalar charge, in equatorial circular orbits, with radius a and angular velocity Ω . This source term S obeys the symmetry property that is necessary if a periodic solution is to exist: its Lie derivative vanishes along the Killing orbit $\vec{\xi}$.

If we are interested only in helically symmetric solutions, then the field equation (3) reduces to

$$\frac{1}{r^2} \frac{\partial}{\partial r} \left(r^2 \frac{\partial \Psi}{\partial r} \right) + \frac{1}{r^2 \sin \theta} \frac{\partial}{\partial \theta} \left(\sin \theta \frac{\partial \Psi}{\partial \theta} \right) + \left[\frac{1}{r^2 \sin^2 \theta} - \Omega^2 \right] \frac{\partial^2 \Psi}{\partial \varphi^2} + \lambda F(\Psi, r, \theta, \varphi) = S(r, \theta, \varphi) . \quad (5)$$

The mixed character of this PDE shows clearly in the coefficient of $\partial_\varphi^2 \Psi$. The light cylinder is at $r \sin \theta = 1/\Omega$ where this coefficient changes sign. Inside the light cylinder ($r \sin \theta < 1/\Omega$) the equation is elliptical; outside it is hyperbolic. For outgoing solutions of this equation we impose an outer boundary condition $\partial_r \Psi = -\partial_t \Psi$, or equivalently $\partial_r \Psi = \Omega \partial_\varphi \Psi$, on a spherical surface with a radius large compared to $1/\Omega$. As illustrated in Fig. 2, this spherical surface is well outside the light cylinder in the equatorial plane, so our boundary conditions are imposed on a surface that passes through both the elliptic and hyperbolic regions of the problem.

Problems with boundary conditions on closed surfaces are common in the case of elliptical PDEs. We argue here that our boundary value problem with mixed PDEs may be unusual, but is well posed. Again, a simple model problem will help to clarify issues. We set the nonlinearity parameter λ to zero in Eq. (5) so that we can solve the resulting linear equation as an infinite series. If we choose a Dirichlet condition

$$\Psi|_{r=r_{\max}} = 0 , \quad (6)$$

at a finite radius r_{\max} , then the solution to this linear problem can be written in terms of spherical Bessel functions j_ℓ, n_ℓ as

$$\Psi = \sum_\ell \sum_{m=\text{even}} \frac{2m\Omega Y_{\ell m}^*(\pi/2, 0) Y_{\ell m}(\theta, \varphi)}{j_\ell(m\Omega r_{\max})} j_\ell(m\Omega r_{<}) [n_\ell(m\Omega r_{>}) j_\ell(m\Omega r_{\max}) - n_\ell(m\Omega r_{\max}) j_\ell(m\Omega r_{>})] . \quad (7)$$

Here $r_{<}(r_{>})$ indicates the smaller (greater) of the quantities r, a . Vanishing of the $j_\ell(m\Omega r_{\max})$ denominator means that the the ‘‘cavity’’ $r \leq r_{\max}$ has a resonant mode at frequency Ω . In the case that r_{\max} has one of the resonant values, the solution to the boundary value problem is not unique. Such values of r are of zero measure, but are dense in the set of all r choices. This means that the cavity is always arbitrarily close to a resonance, if sufficiently high angular modes are computed. A consequence of this is that a numerical computation does not converge. (Computed solutions depend on the computational grid size, and become larger with increasing angular resolution.) The difficulty is not just one of computational practice. The boundary value problem is fundamentally ill-posed as a representation of fields in an infinite space. There is no meaningful $r_{\max} \rightarrow \infty$ limit of Eq. (7).

Problems with mixed elliptic and hyperbolic regions are of some interest in aerodynamics[22], but there are few general results on well-posedness. In those results that do exist, the nature of the boundary conditions plays a pivotal role. We have found that this applies to our periodic solutions also. If we replace the Dirichlet conditions of Eq. (7) with the Sommerfeld condition

$$(\partial_r \Psi - \Omega \partial_\varphi \Psi)|_{r=r_{\max}} = 0 , \quad (8)$$

then the problem is found to be well-posed. This is particularly clear for the linear problem, where the closed form solution takes the form

$$\Psi = \Psi_{\text{out}} + \Psi_{\text{extra}} . \quad (9)$$

Here Ψ_{out} is the usual ‘‘outgoing at infinity’’ solution

$$\Psi_{\text{out}} = \sum_\ell \sum_{m=\text{even}} -2im\Omega Y_{\ell m}^*(\pi/2, 0) Y_{\ell m}(\theta, \varphi) j_\ell(m\Omega r_{<}) h_\ell^{(1)}(m\Omega r_{>}) \quad (10)$$

and

$$\Psi_{\text{extra}} \equiv \sum_{\ell} \sum_{m=\text{even}} -2im\Omega Y_{\ell m}^*(\pi/2, 0) Y_{\ell m}(\theta, \varphi) \gamma_{\ell m} j_{\ell}(m\Omega r_{<}) j_{\ell}(m\Omega r_{>}) \quad (11)$$

with

$$\gamma_{\ell m} \equiv - \left(\frac{h_{\ell}^{(1)}(z) + i dh_{\ell}^{(1)}(z)/dz}{j_{\ell}(z) + i dj_{\ell}(z)/dz} \right)_{z=m\Omega r_{\text{max}}} . \quad (12)$$

Since the spherical Hankel function has the asymptotic form $h_{\ell}^{(1)}(z) = (-i)^{(\ell+1)} e^{iz} [1/z + \mathcal{O}(1/z^2)]$, it follows that $|\gamma_{\ell m}|$ is of order $1/r_{\text{max}}$. Thus, $\Psi \rightarrow \Psi_{\text{out}}$, as $r_{\text{max}} \rightarrow \infty$, suggesting that the linear problem is well posed[23].

Numerical results confirm this suggestion. With the boundary condition in Eq. (8), we have encountered no fundamental difficulty computing convergent solutions to both the linear and nonlinear versions of Eq. (5), and have confirmed that solutions do not depend on the particular (large) value chosen for r_{max} .

Standing waves: iterative method

The solutions we will be computing in Einstein's theory, of course, are standing wave solutions, but there are no actual "standing wave boundary conditions" analogous to the Sommerfeld condition in Eq. (8) for outgoing waves. It is useful, therefore, to explore the meaning of standing-wave solutions with our model nonlinear theories. As pointed out in Sec. I, our paradigm for standing waves is the LSIO of a linear theory, the linear superposition of half ingoing and half outgoing solutions. We shall extend this definition of standing wave to nonlinear theories in two ways. The first is an extension of the Green function method of Ref. [15], and is called there the TSGF (time symmetric Green function) method. For the problem in Eq. (3) this method starts by writing the field equation in the form

$$\mathcal{L}\Psi = \sigma_{\text{eff}}[\Psi]. \quad (13)$$

Here the operator $\mathcal{L}[\Psi]$ depends on Ψ but — once Ψ is fixed — can be considered to be linearly operating on Ψ . Similarly σ_{eff} depends on Ψ , but — once Ψ is fixed — is to be considered a fixed inhomogeneous term in the equation, an effective source term. There is no unique way of putting the field equation into the form of Eq. (13) for a nonlinear model problem, or for general relativity. The quasilinearity of general relativity, and of our nonlinear models, means that at least the principal part of \mathcal{L} is always unambiguous. There are also some obvious guidelines to follow. In particular, \mathcal{L} and σ_{eff} should become Ψ -independent in the weak field limit.

To iterate for an outgoing solution, for example, one would find an approximate outgoing solution Ψ_{out}^n , and then would solve

$$\mathcal{L}[\Psi_{\text{out}}^n](\Psi_{\text{out}}^{n+1}) = \sigma_{\text{eff}}[\Psi_{\text{out}}^n], \quad (14)$$

for outgoing boundary conditions. The result would be the improved approximation Ψ_{out}^{n+1} to the outgoing waves. To find standing waves, this method is modified as follows. An approximation Ψ_{stnd}^n is found to the standing-wave solution. The equation

$$\mathcal{L}[\Psi_{\text{stnd}}^n](\Psi^{n+1}) = \sigma_{\text{eff}}[\Psi_{\text{stnd}}^n], \quad (15)$$

is then solved with the outgoing boundary conditions of Eq. (8) to give $\Psi_{\text{stout}}^{n+1}$ and is next solved with ingoing boundary conditions $\Omega \rightarrow -\Omega$ in Eq. (8) to give Ψ_{stin}^{n+1} . The new approximation for the standing-wave solution is taken to be

$$\Psi_{\text{stnd}}^{n+1} = \frac{1}{2} \Psi_{\text{stout}}^{n+1} + \frac{1}{2} \Psi_{\text{stin}}^{n+1} . \quad (16)$$

We take the $n \rightarrow \infty$ limit of Ψ_{stnd}^{n+1} in Eq. (16) to be our computed standing-wave solution.

We shall call the iterative method just described "direct iteration." This sort of direct iteration is useful in solving for the root of an equation $x = f(x)$ only if f is slowly varying. In iteration for Ψ the equivalent condition applies to $\mathcal{L}^{-1} \circ \sigma_{\text{eff}}$, where \mathcal{L}^{-1} is the Green function, the inverse of \mathcal{L} for the boundary conditions (ingoing or outgoing) of interest. For direct iteration to converge the dependence of $\mathcal{L}^{-1} \circ \sigma_{\text{eff}}$ on Ψ must be weak and this is the case only for nonlinearities of moderate strength. For strong nonlinearities another technique must be used.

In Newton-Raphson iteration, one uses the iteration Ψ^n to make linear approximations for \mathcal{L} and σ_{eff} . Equation (13) then takes the form

$$\mathcal{L}[\Psi^n](\Psi) + (\Psi - \Psi^n) \times \left[\frac{\partial \mathcal{L}[\Psi]}{\partial \Psi} \right]_{\Psi=\Psi^n} (\Psi^n) = \sigma_{\text{eff}}[\Psi^n] + (\Psi - \Psi^n) \times \left[\frac{\partial \sigma_{\text{eff}}}{\partial \Psi} \right]_{\Psi=\Psi^n} . \quad (17)$$

This equation is linear in Ψ , and its solution is taken to be the next iteration Ψ^{n+1} . By choosing appropriate boundary conditions we can use this scheme to iterate an outgoing or ingoing solutions. For our standing-wave solution, we follow the same general scheme as with direct iteration. Using the n^{th} standing-wave approximation as Ψ^n in Eq. (17) we solve using both in- and outgoing boundary conditions. As in Eq. (16), the $n + 1^{\text{th}}$ standing-wave approximation is taken to be half the sum of the ingoing and outgoing solutions found this way.

Standing waves: minimization method

To explain our second, independent way of defining and computing standing-wave solutions, it is best to start with the standing-wave solution in the linear model problem. This is simply half the sum of the “outgoing at infinity” solution in Eq. (10), and the equivalent ingoing solution. The result is

$$\Psi_{\text{std}} = \sum_{\ell} \sum_{m=\text{even}} 2m\Omega Y_{\ell m}^*(\pi/2, 0) Y_{\ell m}(\theta, \varphi) j_{\ell}(m\Omega r_{<}) n_{\ell}(m\Omega r_{>}) . \quad (18)$$

In this solution each multipole has an equal amplitude for ingoing and outgoing amplitudes waves, and one might suspect that this property suffices to define standing waves for a nonlinear model. This is not, in fact the case, since we could add a multiple of the homogeneous solution $j_{\ell}(m\Omega r) j_{\ell}(m\Omega a)$ to the ℓ, m mode without changing the balance between ingoing and outgoing. This degree of freedom is equivalent to the degree of freedom inherent in the phase between the outgoing and ingoing waves. This extra degree of freedom exists also (though not so transparently) in a nonlinear problem.

To resolve this degree of freedom we can use a generalization of a property that is unique, in the linear case, to the correct standing-wave solution Eq. (18): In each multipole, the solution is required to have the minimum wave amplitude of any solution with balanced ingoing and outgoing waves[24].

This method, while very interesting in principle, is difficult in practice to implement in a finite difference boundary value approach. One could imagine using a guess for the value of a multipole coefficient at some outer boundary, and then searching for the value that gives the minimum for the amplitudes of the waves in that multipole. In a nonlinear problem, the values of each multipole will influence other multipoles, so the search for minimum waves will, in principle, be a search in a many dimensional space.

The real difficulty of this numerical approach is that it uses multipoles as part of the boundary condition. That means that multipole coefficients must be extracted. Even in spherical coordinates, the extraction of the multipole coefficients involves a weighted sum over all angular grid points. Most important, this sum would not be performed as a postprocessing step on a computed solution, but rather would have to be written as a set of equations that would form part of the *a priori* problem to be solved. The set of equations to be solved would then have, in addition to great complexity, a boundary-related subset connecting distant grid points. The matrix representation of these equations would not have banded structure. In addition to these technical difficulties, the use of spherical coordinates is very ill suited to the structure of our source objects, so coordinate patches for the sources would be required.

For these reasons, we have not attempted to use the minimization criterion in a finite difference code. We have, however, implemented this criterion with a spectral approach based on a specially adapted coordinate system. Results from this approach are extremely encouraging, but the approach poses new computational challenges, so we are continuing to explore two distinct paths: finite difference methods and the iterative definition of standing waves, and a spectral/adapted coordinate technique for the minimization criterion. Since the adapted coordinate system necessary for the second approach requires a separate development, and is not fundamental to the PSW approximation, we confine the present discussion to the first approach, finite difference boundary value problems, with the iterative criterion for standing waves.

III. NUMERICAL IMPLEMENTATION AND RESULTS

Extraction of an outgoing approximation

Model problems allow us to test a key idea of the PSW approach, that a good approximation of the outgoing solution can be extracted from the computed standing-wave solution

$$\Psi_{\text{stdcomp}} = \sum_{\text{even } \ell} \sum_{m=0, \pm 2, \pm 4..} \alpha_{\ell m}(r) Y_{\ell m}(\theta, \varphi) . \quad (19)$$

The coefficients $\alpha_{\ell m}(r)$ are computed from Ψ_{comp} , by projection with $Y_{\ell m}^*$. From the reality of Ψ_{stdcomp} , the coefficients will obey $\alpha_{\ell m}^* = \alpha_{\ell -m}$, and from the standing-wave symmetry ($\cos m\varphi$ only, no $\sin m\varphi$ terms) they will also obey $\alpha_{\ell m} = \alpha_{\ell -m}$.

This form of the computed standing-wave solution is compared with a general homogeneous linear ($\lambda = 0$) standing-wave (equal magnitude in- and outgoing waves) solution of Eq. (5), with the symmetry of two equal and opposite sources:

$$\Psi_{\text{stdlin}} = \sum_{\text{even } \ell} \sum_{m=0, \pm 2, \pm 4..} Y_{\ell m}(\theta, \varphi) \left[\frac{1}{2} C_{\ell m} h_{\ell}^{(1)}(m\Omega r) + \frac{1}{2} C_{\ell m}^* h_{\ell}^{(2)}(m\Omega r) \right], \quad (20)$$

where $C_{\ell -m} = C_{\ell m}^*$, from the reality of Ψ_{stdlin} . A fitting, in the weak-field zone, of this form of the standing-wave multipole to the computed function $\alpha_{\ell m}(r)$ gives the value of $C_{\ell m}$.

By viewing the linear solution as half-ingoing and half-outgoing we define the extracted outgoing solution to be

$$\Psi_{\text{exout}} = \sum_{\text{even } \ell} \sum_{m=0, \pm 2, \pm 4..} Y_{\ell m}(\theta, \varphi) C_{\ell m} h_{\ell}^{(1)}(m\Omega r). \quad (21)$$

Since this extracted solution was fitted to the computed solution assuming only that linearity applied, it will be a good approximation except in the strong-field region. In the problems of interest, the strong-fields should be confined to a region near the sources. In those regions, small compared to a wavelength, the field will essentially be that of a static source, and will be insensitive to the distant radiative boundary conditions. As pointed out in Sec. I, the solutions in this region will be essentially the same for the ingoing, outgoing, and standing-wave problem. In this inner region then, we take our extracted outgoing solution simply to be the computed standing-wave solution, so that

$$\Psi_{\text{exout}} = \begin{cases} \sum Y_{\ell m} C_{\ell m} h_{\ell}^{(1)} & \text{weak field outer region} \\ \Psi_{\text{stdcomp}} & \text{strong field inner region} \end{cases}. \quad (22)$$

The boundary between a strong field inner region and weak field outer region would ideally be a closed surface surrounding each of the source regions. This is easily implemented with the adapted coordinates to be introduced in a subsequent paper. Here, for simplicity, we take the boundary to be a spherical surface around the origin. In order for the extracted solution to be smooth at this boundary, we use a blending of the inner and outer solution in a transition region extending between radii r_{low} and r_{high} and, in this region, we take

$$\Psi_{\text{exout}} = \beta(r) \sum Y_{\ell m} C_{\ell m} h_{\ell}^{(1)} + [1 - \beta(r)] \Psi_{\text{stdcomp}}. \quad (23)$$

Here

$$\beta(r) \equiv 3 \left[\frac{r - r_{\text{low}}}{r_{\text{high}} - r_{\text{low}}} \right]^2 - 2 \left[\frac{r - r_{\text{low}}}{r_{\text{high}} - r_{\text{low}}} \right], \quad (24)$$

so that $\beta(r)$ goes from 0 at $r = r_{\text{low}}$ to unity at $r = r_{\text{high}}$ and has a vanishing r -derivative at both ends.

In the case of our typical choice $\Omega = 0.3$, the value of r_{low} is chosen to be $r = 1.3a$ the value at which the static and standing-wave solutions of the linear problem differ by 10%. This value should decrease with increasing Ω , but it must be larger than the orbital radius $r = a$, so we choose it to be

$$r_{\text{low}} = a[1 + 0.3(0.3/\Omega)]. \quad (25)$$

In order to have a moderately thin transition region we somewhat arbitrarily take

$$r_{\text{high}} = a[1 + 0.6(0.3/\Omega)]. \quad (26)$$

For the numerical results reported below, the extraction details of Eqs. (19)–(26) are used, and extraction is carried out using the $\ell = 0, 2, 4$ multipoles.

Choice of models

To verify and demonstrate several innovative features (well-posed mixed boundary value problem, standing waves, effective linearity) of the PSW approximation, we use the nonlinear scalar model of Eq. (5), with the delta function

sources given by Eq. (4). We make the simplifying assumption that the nonlinear function F in Eq. (5) depends only on Ψ , not on its derivatives. From this an obvious simplification follows for the iteration method of Eqs. (13) – (16).

We replace Eq. (13) by

$$\mathcal{L}(\Psi) = \sigma_{\text{eff}}[\Psi]. \quad (27)$$

with \mathcal{L} taken to be

$$\mathcal{L} \equiv \frac{1}{r^2} \frac{\partial}{\partial r} \left(r^2 \frac{\partial}{\partial r} \right) + \frac{1}{r^2 \sin \theta} \frac{\partial}{\partial \theta} \left(\sin \theta \frac{\partial}{\partial \theta} \right) + \left[\frac{1}{r^2 \sin^2 \theta} - \Omega^2 \right] \frac{\partial^2}{\partial \varphi^2}. \quad (28)$$

The effective source term includes both the true point source and the nonlinear term

$$\sigma_{\text{eff}}[\Psi] = \frac{\delta(r-a)}{a^2} \delta(\theta - \pi/2) [\delta(\varphi) + \delta(\varphi - \pi)] - \lambda F. \quad (29)$$

Since \mathcal{L} is independent of Ψ we can (as in Ref. [15]) compute once and for all the inverses of \mathcal{L} , i.e., the Green functions corresponding to specific boundary conditions. In this way, we can compute $\mathcal{L}_{\text{out}}^{-1}$ and $\mathcal{L}_{\text{in}}^{-1}$, the Green functions, respectively for outgoing and for ingoing boundary conditions. The direct iterative method of Eqs. (14) – (15), then amount to

$$\Psi_{\text{out}}^{n+1} = \mathcal{L}_{\text{out}}^{-1} (\sigma_{\text{eff}}[\Psi_{\text{out}}^n]) \quad \Psi_{\text{in}}^{n+1} = \mathcal{L}_{\text{in}}^{-1} (\sigma_{\text{eff}}[\Psi_{\text{in}}^n]) \quad (30)$$

$$\Psi_{\text{std}}^{n+1} = \frac{1}{2} \{ \mathcal{L}_{\text{out}}^{-1} + \mathcal{L}_{\text{in}}^{-1} \} \sigma_{\text{eff}}[\Psi_{\text{std}}^n]. \quad (31)$$

Since \mathcal{L} has no Ψ dependence, the basic Newton-Raphson iteration simplifies to

$$\left\{ \mathcal{L} - \left[\frac{\partial \sigma_{\text{eff}}}{\partial \Psi} \right]_{\Psi=\Psi^n} \right\} \Psi = \sigma_{\text{eff}}[\Psi^n] - \Psi^n \left[\frac{\partial \sigma_{\text{eff}}}{\partial \Psi} \right]_{\Psi=\Psi^n}. \quad (32)$$

This basic iteration is applied to the outgoing, ingoing and standing-wave solutions.

As already mentioned following Eq. (5), the most natural choice for the nonlinear term F is a choice like $F = \Psi^3/(1 + \Psi^2)$ which has no explicit dependence on coordinates. We will, however, want to make an important point below about the role of the nonlinear region, the region in which the nonlinearity is strong. In doing this, it will be convenient for us to use the distance R_+ (R_-) from the source point on the x axis at $x = a$ ($x = -a$), given by

$$R_{\pm}^2 = (r \sin \theta \cos \varphi \mp a)^2 + r^2 \sin^2 \theta \cos^2 \varphi + r^2 \cos^2 \theta. \quad (33)$$

In terms of these we introduce the distance variable

$$\chi \equiv \sqrt{R_+ R_-}. \quad (34)$$

At either of the source points $\chi \rightarrow 0$, and far from the sources $\chi \rightarrow r$. We will take our nonlinearity to have the form[25]

$$F = \left(\frac{\chi}{na} \right)^n e^{(n-\chi/a)} \frac{\Psi^3}{1 + \Psi^2}. \quad (35)$$

The choice of n in the χ -dependent prefactor determines where the nonlinearity will be strongest. In particular, a large value of n can put the nonlinearity in the wave zone.

Numerical methods

Each iteration of Eqs. (30) or (31) is equivalent to the solution of a large set of linear equations. Such systems are most typically encountered for elliptic boundary value problems, and are typically solved most efficiently with relaxation methods, or related methods (e.g., multigrid) based on the geometry of the problem. Such methods start with an approximate set of values for each of the unknowns at every point of the numerical grid. At each point the solution is then recalculated on the basis of the values at nearby grid points. This method sweeps through all the points of the grid and is iterated until an error criterion is met. Such a method must be compatible with the domain of dependence for the points of the grid. For an elliptic PDE, for example, the values of unknowns are

updated at a central point of a set of grid points. For a hyperbolic PDE, updated values must be assigned to a point in the “future” of those grid points being used. For a mixed boundary value problem a relaxation method has special problems, especially at the interface between elliptic and hyperbolic regions. Nevertheless, relaxation methods have been successfully applied to mixed PDEs in transonic aerodynamics, first by Murman and Cole[26]. The slow convergence of this method at the interface (the “sonic surface” in transonic aerodynamics) can be improved with special techniques that may need to be specific to the problem[27].

We are presently investigating relaxation and other numerical methods (e.g., decomposing the grid into regions and applying different techniques, preconditioners, etc.) for large grids and many variables. For our three-dimensional scalar problem illustrated here, however, we have been able to use a more-or-less straightforward method of inverting the matrix for the finite difference equations. In one approach we use this matrix inversion at each step of the direct iteration of Eqs. (30), (31), and we take advantage of the rotational symmetry (i.e., the translational symmetry with respect to φ) of \mathcal{L}^{-1} . At each step of iteration we decompose $\Psi^{n+1}(r, \theta, \varphi)$ into its Fourier components $\Psi_m^{n+1}(r, \theta)e^{im\varphi}$ and we project out the Fourier components of the effective source. Due to the symmetry of \mathcal{L}^{-1} the Fourier modes of Ψ^{n+1} do not mix. This method takes advantage of the efficiency of a fast Fourier transform (FFT) and reduces the RAM needed to that for the modest requirements of a two-dimensional r, θ grid.

We have used this efficient FFT method extensively, but direct iteration has the drawback already cited: it is limited in the strength of the nonlinearity it can handle. Direct iteration will not converge for very strong nonlinearity. The iterative Newton-Raphson method of Eq. (32), on the other hand, does almost always converge once one has a solution sufficiently close to the correct solution. The operator on the left in Eq. (32), however, contains the previous iteration Ψ^n , which is not symmetric in φ , so that the FFT method cannot be used. This has meant that a relatively coarse grid, or large RAM had to be used. We have not yet implemented a parallelizable method for solving the iteration steps, so the extent to which “large RAM” could be used has been limited.

A practical difficulty with the very strongly nonlinear models has been the need to get close enough to the correct solution for Newton-Raphson convergence to take effect. This has been done by using continuation in λ . A solution is easily found for a sufficiently small value of λ . That solution is then used as the starting point for iteration with a larger value of λ , and in this way we can “ramp up” to relatively large values of λ . It has also been found effective to continue in Ω .

Numerical results

We first illustrate the fundamental concept of the PSW method with various solutions of Eq. (5), with the nonlinearity given in Eq. (35). Figure 3 shows solutions in the equatorial ($\theta = \pi/2$) plane; the amplitude of the field Ψ is plotted as a function of corotating Cartesian coordinates x, y with $x = r \cos \varphi$, and $y = r \sin \varphi$. The source points are on the x axis at $x = \pm a$. For all four plots, $a\Omega = 0.3$, $\lambda = -20$, and $n = 0$ (that is, the prefactor in Eq. (35) is taken to be $e^{-\chi/a}$). For these parameters the nonlinearity is nonnegligible, but is sufficiently weak that direct iteration converges, and the efficiency of the FFT method can be exploited. The r, θ, φ grid resolution for these computations is $720 \times 32 \times 128$. For all models, the computed results are dominated by the monopole, so for clarity in the figures the φ -average of the solution has been subtracted at every radius. It is worth noting that this procedure not only removes the monopole (the $\ell = 0$ part of the solution), but also removes the $m = 0$ part of the quadrupole, etc.

The plot in part (a) of Fig. 3 shows the outgoing solution (solution for outgoing boundary conditions); the plot in part (b) shows the corresponding ingoing solution. The plot in part (c) is the computed standing-wave solution for the same problem parameters. (Note: this nonlinear standing-wave solution is *not* half the superposition of the outgoing and ingoing solutions. Rather, it is the nonlinear field equation solved with the standing-wave definition discussed in Sec. II.) Part (d) shows the key idea of the PSW approximation, the outgoing solution extracted from the standing-wave solution, by the extraction method described in Eqs. (19)–(26). When the PSW method is used in general relativity, it will be possible only to compute the standing-wave solution; the extracted outgoing solution will represent the approximation to the physical, outgoing solution.

In Fig. 3 we can see only that this extracted outgoing solution is qualitatively a good approximation to the $n = 0$ true outgoing solution of part (a). For the quantitative results underlying those figures, a verbal description turns out to be better than a graphical one. In particular, one of the conceptual foundations of effective linearity is that the solution near the strong-field sources does not depend on the radiation boundary conditions. With $a\Omega = 0.3$, with nonlinearity parameter $n = 0$ in Eq. (35), and with radiative boundary conditions at $r = 30a$, models that we have computed could not produce more than a few percent difference between the ingoing/outgoing solution and the standing-wave solution in the region within a distance $0.5a$ in any direction of the source location at $x = \pm a$ in the equatorial plane. These differences are smaller than the truncation errors in the computation.

This turns out, in fact, to be true for the whole computational domain. For the ($n = 0$, $a\Omega = 0.3$, outer boundary at $30a$) model shown in Fig. 3, Newton-Raphson iteration, and careful ramping in λ allowed us to reach $\lambda = -70$,

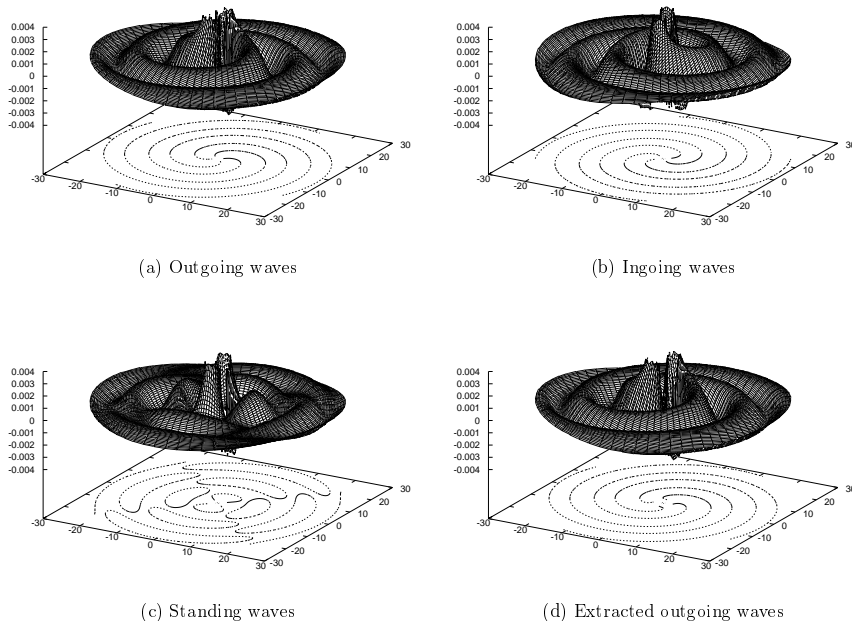


FIG. 3: The Ψ field for two rotating point sources in the equatorial plane. The fields shown are nonlinear solutions of Eqs. (4), (5) and (35), with $a\Omega = 0.3$, $n = 0$ and $\lambda = -20$. For clarity, the φ -average is removed at each radius. Parts (a) and (b) of the figure show, respectively, the nonlinear outgoing and ingoing solutions. Part (c) is the standing-wave solution, and part (d) is the outgoing solution extracted from it. The vertical scale gives field strength (arbitrary units) and the horizontal coordinates are corotating Cartesian coordinates in units of a , the distance of a source from the rotation axis.

for which results are presented as part (a) in Fig. 4. The curves show the solutions along an outgoing radial line through the source points, i.e., the radial line at $\theta = \pi/2$, $\varphi = 0$. Plotted in that figure are the extracted nonlinear outgoing solution (short dashes), the true nonlinear outgoing solution (long dashes), and — to indicate the size of the nonlinear effect — the linear solution (solid curve) for the same value of $a\Omega$ and outer boundary. Though the effect of the $\lambda = -70$, $n = 0$ nonlinearity is to increase the wave amplitude by a factor of almost four, there is a negligible difference between the true outgoing solution, and the extracted outgoing solution; the difference is on the same order as the truncation error. In this plot, then, the PSW approximation appears to be essentially perfect.

To some extent this apparent perfection is a statement about the limits of the numerical method used here. Even with the strong-nonlinearity techniques described above (Newton-Raphson iteration and ramping in λ) models with extremely strong nonlinearity cannot be run. It is important, nevertheless, to show that the PSW approximation is only an approximation, and to exhibit its limitations. To force the PSW approximation to fail, we recall that effective linearity is based on the fact that the strong-field region is confined near the sources where the solution is insensitive to the radiative boundary conditions. By taking relatively large values for the parameter n of Eq. (35) we push the strong nonlinearity (the strongest for which we can get a convergent iteration) out near the wave zone where the solution *is* sensitive to the radiative boundary conditions.

The results of this exercise are shown as parts (b) and (c) of Fig. 4. All solutions are for $a\Omega = 0.3$, with radiative boundary conditions at $r = 30a$, but values $n = 5$ and $n = 10$ are used. For each of the models, Newton-Raphson iteration was used, and the magnitude of λ was ramped up to the maximum value for which iteration converged. Different maximum values of λ were reached for the different n values, but in any case the relationship of λ to the strength of the nonlinearity is different in each model. A more meaningful indication of the strength of the nonlinearity is the difference between the nonlinear model and the corresponding linear model shown in each case.

For the $n = 5$ and 10 cases, the strength of the nonlinearity is not as strong as in the $n = 0$ case, but there are larger errors in the PSW approximation; the differences between the true outgoing and extracted outgoing waves are larger. The effective linearity viewpoint is therefore supported: the PSW approximation is accurate to the extent that nonlinearity does not overlap the (boundary-condition sensitive) wave zone.

A few features of the results in Fig. 4 deserve comment. First, it should be noted that for large r the agreement is excellent between the true outgoing waves and extracted outgoing waves. This is equivalent to the statement that the LSIO, the superposition of the true nonlinear outgoing and true nonlinear ingoing solutions, is almost a solution in the weak-field large- r region, and is an excellent approximation to the computed standing-wave solution. This fact

is not affected by the nonlinearities at smaller r . A second obvious feature of the solution concerns phase shifts. For $n = 0$, despite the strength of the nonlinearity, there is no obvious phase difference in the wave zone between the linear and nonlinear results. In contrast, there is significant phase shift for the $n = 5$ and 10 models. A phase shift is lacking in the $n = 0$ case because the nonlinearity, confined near the sources, acts as if it were amplifying the sources. That is, it creates a strong field, that itself is a source, at the same location as the actual source, and with no phase lag. On the other hand, in the large n solutions, the the strong field regions that are acting as a sources, are not at the same φ location as the actual sources. The radiation from these effective sources is not in phase with that from the actual sources.

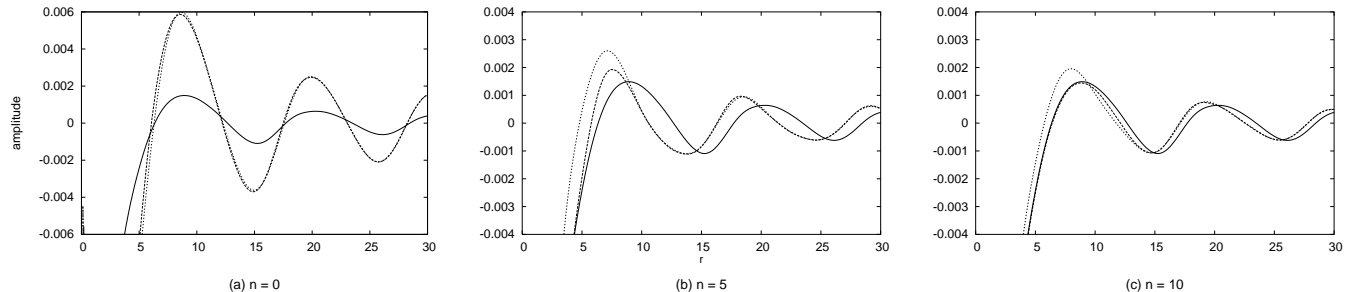


FIG. 4: Linear and nonlinear outgoing solutions, at $\varphi = 0$ in the equatorial plane, all for $a\Omega = 0.3$, with radiative boundary conditions at $r = 30a$. Solid curves show the linear (i.e., $\lambda = 0$) solution; the nonlinear outgoing solution is shown with long dashes. The curve with short dashes shows the outgoing solution extracted from the standing-wave solution. The three models correspond to the different distributions of nonlinearity given by $n = 0, 5$ and 10.

The χ -dependent factors with which we forced the nonlinearity into the wave zone are, of course, unphysical. In the problem of physical interest, compact binaries, what could make the basis of effective linearity fail is very relativistic motion of the binary objects; for $a\Omega \approx 1$ the wave zone starts right at the orbital radius. This is implausible in general relativistic binary models. If a highly relativistic orbit were possible, the radius would quickly decrease due to loss in gravitational waves, and the periodic approximation would be inapplicable. For our scalar model, however, it is possible in principle to increase $a\Omega$, and see the onset of failure of the PSW. In practice, this could not be done with the straightforward numerical approach reported on here. For $a\Omega$ larger than 0.3, the waves have significant contributions from $\ell > 2$ multipoles. We are limited to 32 divisions of φ to cover the range of φ from 0 to π (with symmetry giving π to 2π). This is too coarse a grid to resolve the higher multipoles, and numerical artifacts develop in the extracted waveform. (That φ resolution is the source of the trouble was checked by running linear models with the large resolution available through the FFT method. The numerical artifacts did appear in the linear models, and disappeared when φ resolution was increased.)

IV. CONCLUSIONS

We have given here the foundations of the PSW method based on the extraction of an outgoing solution from a computed standing-wave solution. We have also given the details of the extraction calculation.

The results provided for convergent nonlinear models are “proof” by example that there is no fundamental mathematical problem of well-posedness of the mixed PDE problem, with radiative boundary conditions on a sphere that is in both the elliptic and hyperbolic regions of the problem. We have, furthermore, presented limited numerical evidence for the validity of the PSW method, i.e., that the extracted outgoing solution is a good approximation to the true nonlinear outgoing solution. In addition, with somewhat artificial models of nonlinearity, we have bolstered the evidence for the effective linearity that justifies the the PSW approximation. This evidence helps makes the case for the application of the method to the general relativistic problem, in which only the standing-wave solution will be computable, and the extracted solution will be taken as the approximation to the physical problem.

The numerical studies have also taught a lesson about the straightforward numerical method used here, matrix inversion of the finite difference equations in spherical coordinates. We have found that this method is limited in the strength of nonlinearity for which convergent solutions can be found. We could, in principle, use a software engineering approach to increase the range of problems we could handle; we could, for example, use greater RAM and more careful ramping in λ . But the methods used here, spherical coordinates and delta function sources, are meant only to provide a relatively simple context for establishing the foundations for more advanced approaches.

In a paper now in preparation[19], we will present an important step forward in dealing with PSW problems, a coordinate system that conforms to the geometry near the sources and asymptotically goes to spherical polar

coordinates in which the waves are best described. One advantage of this method is that it allows us very simply to put in details of the source as inner boundary conditions rather than point sources. Another, is that it turns out to be very well suited to a spectral method that has shown remarkable computational efficiency, but that poses new computational problems. Computations using an adapted coordinate system have already been carried out for the three-dimensional nonlinear scalar problem with both the finite difference and spectral formulation, and for linearized general relativity using the finite difference formulation. Since the details of adapted coordinates, especially with the unusual spectral method, are not directly related to the foundations of the PSW method, those details are appropriate to a separate paper.

A very different approach to better numerics is to use relaxation methods, already mentioned in Sec. III. In view of the large number of uncertainties about their application, we have started on a basic study of relaxation methods in mixed PDE systems in PSW-type problems.

V. ACKNOWLEDGMENT

We gratefully acknowledge the support of the National Science Foundation under grants PHY9734871 and PHY0244605. We also thank the University of Utah Research Foundation for support during this work. The Supercomputer used in this investigation was provided by funding from JPL Institutional Computing and Information Services and the NASA Offices of Earth Science, Aeronautics, and Space Science. We thank John Friedman and Kip Thorne for helpful discussions and suggestions, and we thank Rachel Costello for contributions to graphical aspects of this work.

-
- [1] G. Gonzalez, gravitational wave detectors: A report from LIGO-land, in *Recent Developments in Gravity: Proceedings of the 10th Hellenic Relativity Conference*, K. D. Kokkotas and N. Stergioulas (Eds.), (World Scientific, Singapore, 2003); [gr-qc/0303117]
 - [2] F. Acernese *et al.*, *Class. Quant. Grav.* **20**, 609 (2003).
 - [3] H. Lück *et al.*, in *Gravitational Waves, Third Edoardo Amaldi Conference held in Pasadena, CA 12-16 July, 1999*, S. Meshkov (Ed), AIP Conference Proceedings, Vol. 523 (AIP Press, New York, 2000), pp. 119–127.
 - [4] M. Ando, Current status of the TAMA300 interferometer, prepared for 2nd Workshop on Gravitational Wave Detection, Tokyo, Japan, 19-22 Oct 1999.
 - [5] E. Colbert and A. Ptak, *Astrophys. J. Supp.* **143**, 25 (2002).
 - [6] B. F. Schutz, in *Lighthouses of the Universe – The Most Luminous Celestial Objects and Their Use for Cosmology: Proceedings of the Mpa/Eso/Mpe/Usm Joint Astronomy Conference*, C. K. Chui, R. A. Siuniae, and E. Churazov (Eds.) (Springer-Verlag, New York, 2002), pp. 207–224; [gr-qc/0111095].
 - [7] See <http://lisa.jpl.nasa.gov>.
 - [8] M. A. Scheel *et al.*, *Phys. Rev. D* **66**, 124005 (2002).
 - [9] H.-J. Yo, T. W. Baumgarte, and S. L. Shapiro, *Phys. Rev. D* **66**, 084026 (2002).
 - [10] J. Baker *et al.*, *Phys. Rev. D* **65**, 124012 (2002).
 - [11] J. K. Blackburn and S. Detweiler, *Phys. Rev. D* **46**, 2318 (1992).
 - [12] S. Detweiler, *Phys. Rev. D* **50**, 4929 (1994).
 - [13] J. Friedman, private communication.
 - [14] C. W. Misner, K. S. Thorne and J. A. Wheeler, *Gravitation* (Freeman, San Francisco, 1973), Sec. 20.3.
 - [15] J. T. Whelan, W. Krivan, and R. H. Price, *Class. Quant. Grav.* **17**, 4895 (2000).
 - [16] A. Ashtekar *et al.*, *Phys. Rev. Lett.* **85**, 3564 (2000).
 - [17] J. W. York, Jr., *Phys. Rev. Lett.* **26**, 1656 (1971).
 - [18] J. W. York, Jr., *J. Math. Phys.* **14**, 456 (1973).
 - [19] Z. Andrade *et al.*, paper in preparation.
 - [20] G. W. Gibbons and J. M. Stewart, in *Classical General Relativity*, edited by W. B. Bonnor, J. N. Islam, and M. A. H. MacCallum (Cambridge University Press, Cambridge, 1983), pp. 77–94.
 - [21] J. L. Friedman, K. Uryu, and M. Shibata, *Phys. Rev. D* **65**, 064035 (2002).
 - [22] C. Ferrari and F. G. Tricomi, *Transonic Aerodynamics* (Academic Press, New York, 1968); J. D. Cole and L. P. Cook, *Transonic Aerodynamics* (North-Holland, Amsterdam, 1986).
 - [23] This is an expanded version of an argument given in the two-dimensional context in Ref. [15].
 - [24] J. T. Whelan, C. Beetle, W. Landry, and R. H. Price, *Class. Quant. Grav.* **19**, 1285 (2002).
 - [25] The exponential localization terms here differ from, and are more realistic than, those used in the two-dimensional models of Ref. [15]. In that work the nonlinearities were localized near the coordinate origin.
 - [26] E. M. Murman and J. D. Cole, *AIAA J.* **9**, 114 (1971).
 - [27] D. Nixon, in *Computational methods and problems in aeronautical fluid dynamics*, edited by B. L. Hewit (Academic Press, New York, 1976), pp. 290–326.